

## A RELATIVISTIC JET IN THE RADIO-QUIET QUASAR PG 1407+263

KATHERINE M. BLUNDELL<sup>1</sup>, ANTHONY J. BEASLEY<sup>2</sup> AND GEOFFREY V. BICKNELL<sup>3</sup>  
*Accepted by ApJ Letters*

## ABSTRACT

We present the results of a multi-epoch radio monitoring campaign measuring the milliarcsecond structure of the jet in the radio-quiet quasar PG 1407+263. This is the highest-sensitivity, highest-resolution multi-year study of a distant active galaxy. The observations are naturally explained in terms of a beamed relativistic jet, some of whose fluctuations in flux density can be ascribed to interaction with the narrow-line region of the quasar. The optical properties of PG 1407+263, in particular the low equivalent widths of the emission lines, may be related to the fact that we are viewing this quasar almost pole-on, giving us a direct view into its broad-line region.

*Subject headings:* galaxies: jets — quasars: individual (PG1407+263) — radio continuum: galaxies

## 1. INTRODUCTION

In recent years, the weak radio core emission associated with the class of so-called ‘radio-quiet’ quasars (for example, Kellermann et al 1989; Miller et al 1990, 1993) has been shown by a succession of Very Long Baseline Interferometry (VLBI) imaging experiments usually to be compact on milliarcsecond (mas) scales (Blundell et al 1996; Falcke, Patnaik & Sherwood 1996; Blundell & Beasley 1998a). The typical physical size of  $\lesssim$  a few cubic parsecs for these radio luminosities and corresponding brightness temperatures ( $> 10^6$  K) strongly argues against star-formation as the origin of this radio emission, despite the striking continuity of the correlation of far-infrared and radio emission from star-forming galaxies to radio-quiet quasars (Sopp and Alexander 1991a,b). Instead, a mechanism resembling that which powers the core emission in the more radio-luminous ‘radio-loud’ quasars is suggested.

One quasar in particular, PG 1407+263, identified in a mas imaging survey of radio-quiet quasars (Blundell & Beasley 1998a) clearly has multiple components and seemed an important target to monitor subsequently with VLBI techniques. It was first discovered as a quasar in the Palomar-Green survey (Schmidt & Green 1983) with  $z = 0.94 \pm 0.02$  (McDowell et al. 1995). With a Hubble constant of  $70 \text{ km s}^{-1} \text{ Mpc}^{-1}$ , and  $(\Omega_M, \Omega_\Lambda) = (0.3, 0.7)$ , the luminosity distance  $\approx 6.2 \text{ Gpc}$  and  $1 \text{ mas} \approx 7.9 \text{ pc}$ .

## 2. MEASUREMENTS

We observed PG 1407+263 at 8.4 GHz using the Very Long Baseline Array (VLBA) with the Very Large Array (VLA) in phased array mode on 1996 June 15 (VLBA only), 1997 April 27, 1998 January 31, 1999 March 20 and 1999 July 20. We usually recorded a 64-MHz bandwidth (a 32-MHz bandwidth was used for epochs 4 & 5) with 2-bit sampling and dual circular polarization. The observations were phase-referenced (Beasley and Conway 1995), i.e. regular observations of a bright extragalactic source close on the sky to the target were made to derive residual antenna-based and atmospheric phase corrections,

which were interpolated to calibrate the target data and provide accurate astrometric referencing. The calibrator source used was OQ 208, separated from PG 1407+263 by  $2.2^\circ$ . We typically used a switching cycle of two minutes on the calibrator and three minutes on the target. The total on-source time for OQ 208 was 0.5 hrs (epoch 1) and 2.8 hrs (epochs 2, 3, 4 and 5). Throughout the three-year monitoring, a pair of  $\lesssim$  mJy components were persistently detected (Figure 1), albeit with changes in structure and flux density (Figure 2).

## 3. LIGHT CURVES AND STRUCTURAL CHANGES

One striking change seen between successive epochs is that the structure of each component appears to vary: this is particularly marked in the final three epochs (Figure 1). Real changes in shape represent an intriguing aspect of the parsec-scale evolution of the source: since 1 mas corresponds to 7.9 pc, real expansion between epochs of one tenth of a synthesized beam would correspond to apparent motion of a few times the speed of light. The components appear both resolved and unresolved at different epochs. Component B appears to be significantly resolved (with a high total flux density) in earlier epochs, while both components appear essentially unresolved (with low flux densities) in the final epoch. Unmodeled residual spatial gradients in tropospheric (and ionospheric) delays lead to interferometer phase errors which are cancelled towards the bright calibrator source OQ 208, but remain in the target data. Thus, apart from the above general assertions above about component B, it is difficult to draw solid conclusions from the structural variations: simple centroid fitting to the components, while technically possible, can be ambiguous in interpretation.

The rms variation of the position of component A is  $\approx 300 \mu\text{-arcsec}$ . Typical estimates of the effects of tropospheric delay errors on phase-referenced VLBI data with a calibrator 2.2 deg away are 100–200  $\mu\text{-arcsec}$ . In addition, the typical signal-to-noise (S/N) of the detections is 5–10 to 1; this would introduce a positional variation roughly equal to the synthesized beam divided by the S/N

<sup>1</sup> University of Oxford, Astrophysics, Keble Road, Oxford, OX1 3RH, UK

<sup>2</sup> Owens Valley Radio Observatory, California Institute of Technology, PO Box 968, Big Pine, CA 93513

<sup>3</sup> Research School of Astronomy & Astrophysics, Australian National University, Canberra, Australia

– i.e. 100 to 250  $\mu$ -arcsec. Therefore, the position wandering largely results from a combination of unmodeled tropospheric delay errors and S/N considerations. Given the weak ( $\lesssim$  mJy) flux density levels in these images, it is not possible to correct for these residual errors. During the course of these observations the relative position shift of components A and B appeared at times to be systematic, possibly indicating superluminal motion (Blundell & Beasley 1998b). Analysis of the existing data set does not allow a definitive determination of superluminal motion in this radio-quiet quasar, although we in any case infer it to have a highly relativistic jet speed (Doppler factor  $\gtrsim 10$ ) in the analysis below. The rapid variations in component B's flux density are unlikely to result from imaging coherence loss, which would affect both components; A's relatively constant peak flux density implies that B's flux density variations are intrinsic. The dramatic changes in B's flux density occur on timescales of 100–300 days, reminiscent of those seen in the cores of radio-loud quasars (Hough et al 1999).

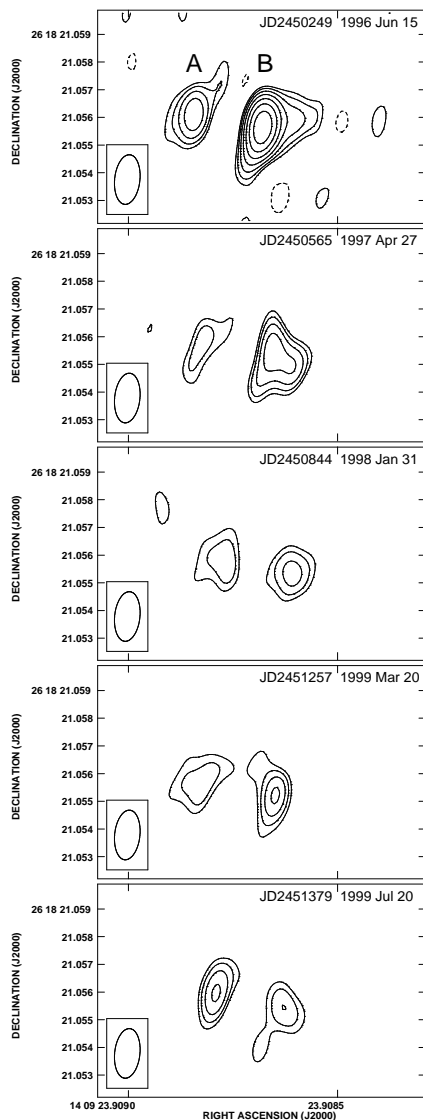


FIG. 1.— VLBA images of PG 1407+263 restored with the same synthesized beam,  $1.8 \times 0.9$  mas with position angle 170 deg East of North. The contours in each case are  $\pm 0.3, 0.42, 0.6, 0.84, 1.2, 1.68, 2.4$  mJy/beam.

#### 4. RECENT RADIO-LOUDNESS OF PG 1407+263

In order to establish whether PG 1407+263 is truly a radio-quiet quasar, we made deep VLA images to search for evidence of extended radio structure or hotspots. These images revealed only independent sources including an apparent double 53 arcsec east of the quasar. Kellermann et al (1989) commented that this double structure might be related to the output of the quasar, since it lacks any optical identification on the Palomar Observatory Sky Survey. We made a more sensitive test by observing the field in the near infra-red *K*-band on the UK Infra-Red Telescope (UKIRT). Figure 3 indicates each part of the ‘double’ radio structure is identified with a galaxy and is thus unrelated to the quasar. Therefore, we do not believe that PG 1407+263 has been radio-loud for the last  $10^6$ – $10^7$  years, where this timescale is taken from the typical radiative lifetimes for synchrotron-emitting particles in the lobes of radio-loud quasars (Blundell & Rawlings 2000).

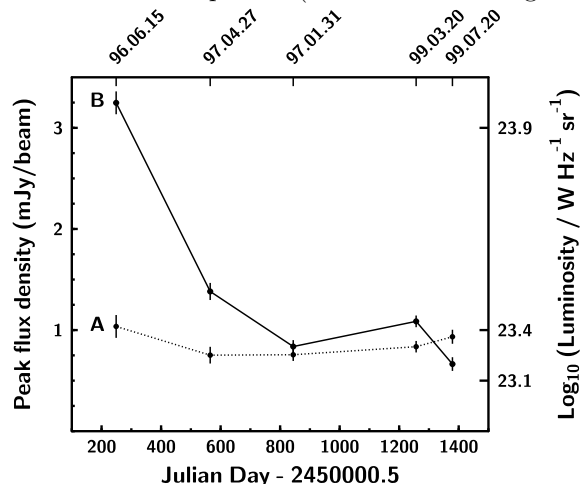


FIG. 2.— Peak flux densities at 8.4 GHz of components A & B at each epoch plotted against time. The dotted line corresponds to the eastern component (A) and the solid line corresponds to the western component (B).

#### 5. PHYSICAL INTERPRETATION

It is feasible that the observed structural changes in component B are related to at least one unresolved sub-component. The much closer source 3C 120 (Gómez et al 2000) is a good example of how jet knot components can appear and fade. Gómez et al have interpreted this in terms of interaction between the jet and the inhomogeneous ambient medium. Observed at lower resolution, the jet in 3C 120 would present apparently structurally changing partially resolved components. If we are indeed observing such a phenomenon, then the offset between the two local surface brightness maxima in component B may give us some idea of the scale of the jet diameter. The perpendicular offset between the centroid of the two B sub-components and the line connecting the two main components, A and B is about  $0.7 \text{ mas} \approx 5.5 \text{ pc}$ . Therefore, in the following, we adopt a fiducial scale for the jet diameter,  $D$  of 5 pc. The causal limit on the diameter deduced from the variability time scale,  $\Delta t$ , and corresponding to a Doppler factor  $\delta$  is:  $D < c(1+z)^{-1} \Delta t \delta \approx 0.4 \left( \frac{\Delta t}{100 \text{ days}} \right) \left( \frac{\delta}{10} \right) \text{ pc}$ . The variation from epochs 1 to 2 entails a factor  $\sim 2$  decrease in flux density over a timescale  $\approx 400$  days. This im-

plies an upper limit on the diameter  $\approx 1.6$  pc for a Doppler factor of 10. This is intriguingly less than, but of the same order as, the approximate scale size estimated from the VLBA images. Of course, the discrepancy decreases with increasing Doppler factor. [If the jet is pole-on so that  $\delta \approx 2\Gamma$  (where  $\Gamma$  is the bulk Lorentz factor), given the existence of apparent proper motions  $\sim 10c$  in some quasars, then  $\delta \sim 20$  is not out of the question.] Clearly, the reconciliation of these two scales is in the direction of larger Doppler factors, not smaller. This is an indication that this source is highly beamed.

A second, more persuasive, indication for beaming comes from estimating the intrinsic source power. The emitted power per steradian is:  $\int j'_\nu dV' = \delta^{-(3+\alpha)} (1+z)^{-(1-\alpha)} F_\nu D_L^2 \text{ W Hz}^{-1} \text{ sr}^{-1}$ , where the integral is that of the rest-frame emissivity,  $j'_\nu$ , at the observed frequency  $\nu$  over the proper volume ( $V'$ ) of each blob and  $F_\nu$  is the flux density at  $\nu$ .

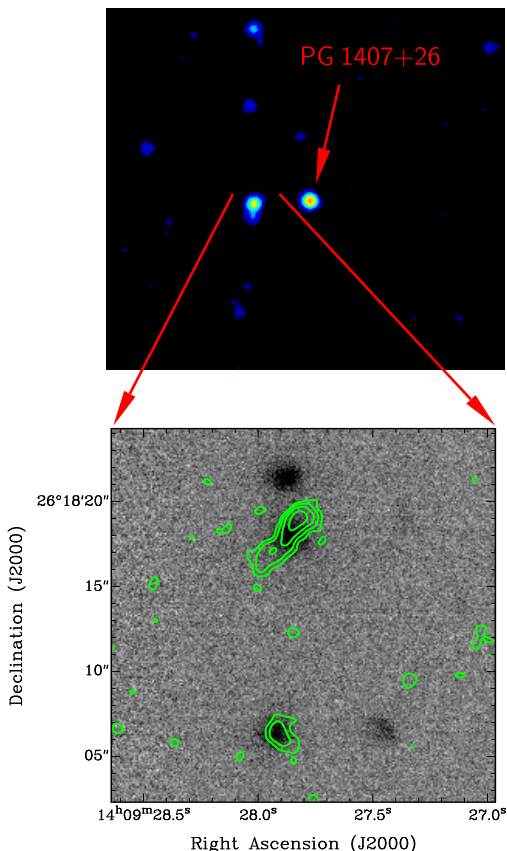


FIG. 3.— The top image is a seven arcmin-square VLA image at 8.4 GHz in D-array. The lower image shows a grey-scale of near-IR  $K$ -band on which are overlaid contours at 8.4 GHz from the VLA A-array, the lowest of which is 0.04 mJy/beam. The two radio sources are clearly identified with resolved 18.5-magnitude galaxies, indicating they are independent radio structures from the quasar.

For unity Doppler factor, the total emitted power, at 8.4 GHz, of both components at epoch 1 would be  $1.1 \times 10^{24} \text{ W Hz}^{-1} \text{ sr}^{-1}$ . This is comparable to the core powers of the most powerful galaxies in the B2 sample (de Ruiter et al 1990). If PG 1407+263 were similar to the B2 sources then, using the statistical relationship between core and extended powers derived by de Ruiter et al (1990), its corresponding 1.4 GHz extended power would be of order  $10^{28} \text{ W Hz}^{-1}$  and the 8.4 GHz flux density

would be of order one Jansky. However, since the flux density of any extended emission from PG 1407+263 is less than 0.1 mJy, this is another indication that the core is beamed. The Doppler factor has to be increased to  $\sim 10$  in order to reduce the expected extended flux density to the observed upper limit. The additional parameters describing each knot are the spectral index  $\alpha$ , the electron energy index,  $a = 2\alpha + 1$ , the volume,  $V'$ , of the knot in its rest frame, the Doppler factor,  $\delta$  and the ratio,  $c_E$ , of energy in relativistic electrons and positrons to other particles. The rest-frame magnetic field that minimizes the total energy density of a spherical blob in the rest frame is:  $B'_{\min} = e^{-1} m_e \delta^{-1} (1+z)^{-\left(\frac{1-\alpha}{\alpha+3}\right)} \times$

$$\left[ (a+1) C_2^{-1}(a) (1+c_E) m_e^{-1} c f(a, \gamma_1, \gamma_2) F_\nu \nu^\alpha D_L^2 V'^{-1} \right]^{\frac{2}{a+5}} \text{ T.}$$

Here  $C_2(a)$  is a coefficient involving  $\Gamma$ -functions that appears in the expression for the angle-averaged synchrotron emissivity;  $e$ ,  $m_e$  and  $c$  are the electronic charge, electronic mass and speed of light respectively, and  $f(a, \gamma_1, \gamma_2) = (a-2)^{-1} \gamma_1^{2-a} (1 - (\gamma_2/\gamma_1)^2)^{-a}$ . We have estimated the minimum-energy magnetic field and corresponding particle energy densities, from the flux density of component B at epoch 1 and for proper jet diameters of 0.375, 0.75 and 1.5 mas as functions of Doppler factor. Figure 4 shows the associated jet energy flux,  $F_E \approx \left[ 4p \left( 1 + \frac{\Gamma-1}{\Gamma} \frac{\rho c^2}{4p} \right) + \left( \frac{B'^2}{\mu_0} \right) \right] \Gamma^2 c \beta A_{\text{jet}}$ , where  $A_{\text{jet}}$  is the cross-sectional area of the jet,  $\rho$  is the rest-mass density, and where the Poynting flux of a perpendicular magnetic field has been included. We assume that the jet is pole-on and purely relativistic, so that  $\rho c^2/4p \ll 1$  and  $c_E = 0$ . The almost constant value of the jet energy flux for Doppler factors  $\geq 2$  is the result of the  $\delta^{-2}$ -dependence of the magnetic and particle energy densities canceling the  $\Gamma^2$ -dependence of the energy flux. If we assume that 0.75 mas is a reasonable upper limit to the jet diameter, then the jet is no more powerful than about  $7 \times 10^{36} \text{ W}$ . For jet diameters less than the fiducial value the jet is less powerful, albeit still relativistic. We note that this is not the first radio-weak object for which relativistic velocities have been inferred. Brunthaler et al. (2000) inferred superluminal motion from their observations of the Seyfert galaxy III Zw 2, directly implying relativistic motion.

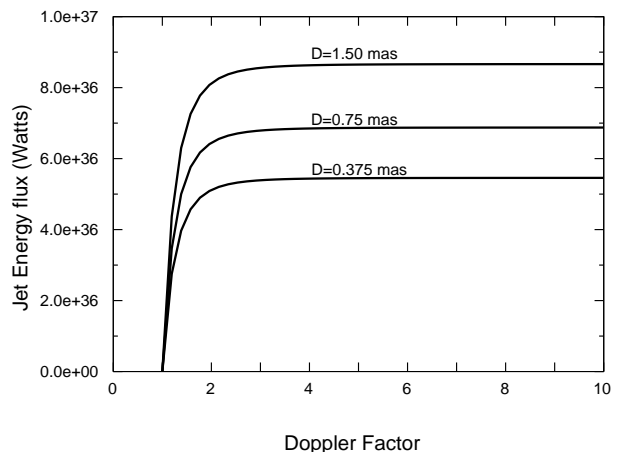


FIG. 4.— Jet energy flux as a function of Doppler factor for three assumed values of the jet diameter: the fiducial jet diameter and a factor of two above and below this.

<sup>4</sup> See <http://www.mso.anu.edu.au/~geoff/HEA/HEA.html>

## 6. DISCUSSION

The low extended emission relative to the core in PG 1407+263 is a good argument that this jet is relativistically beamed. If our inference of partially resolved structure in the jet is correct then the case for relativistic beaming is reinforced by the variability time scale ( $\sim 400$  days for epochs 1-2). If the jet diameter is indeed  $\sim 5$  pc then, given the typical expansion rates of jets, the components are of the order of 100 pc from the core, placing them in the narrow-line region. These two arguments point to a Doppler factor of  $\gtrsim 10$ . As Figure 4 shows, the dependence of energy flux on Doppler factor and jet radius indicates a kinetic power no greater than about  $10^{37}$  W. Using theoretical (Bicknell et al. 1998) and observational (Willott et al 1999) relations between jet and radio power, such an energy flux would be typical of a radio galaxy jet no more than an order of magnitude above the FRI/FRII break (Fanaroff & Riley 1974). The interest that attends this galaxy is the existence of an FRI radio power associated with a bright quasar so it is unsurprising that this quasar is classified as radio quiet (Blundell & Rawlings 2001). It appears the only reason that we detect any radio flux is that it is one of the few PG quasars that is beamed towards us.

As well as its variation between epochs 1 and 2, component B also exhibits a significant rise in flux density  $F_\nu$  between epochs 3 and 4 then a sharp drop ( $\Delta t = 122$  days) between epochs 4 and 5 with  $\Delta F_\nu/F_\nu \sim 1$ . This variability indicates a diameter  $\leq 0.5(\delta/10)$  pc for component B around this epoch – much less than the indicative jet diameter  $\sim 5$  pc inferred above. There are two possibilities: (1) the jet may not be as wide as 5 pc or (2) the variation is

due to a small section of the jet being affected by its interaction with clouds in the narrow-line region of the quasar. This second case is similar to what has been observed in 3C 120 by Gómez et al (2000). Our observations therefore suggest a relativistic jet, of only moderate power, propagating through the clumpy narrow-line region of a bright host quasar.

Does our consideration of the radio structure of PG 1407+263 shed any light on its curious optical properties e.g., the low equivalent width of the emission lines (McDowell et al. 1995)? If the Doppler factor of the jet is as high as 10, then we are viewing PG 1407+263 within a few degrees of pole-on and looking directly into its broad-line region. Thus, the emission line spectrum may be diluted by a direct line of sight to the accretion disk continuum. An argument against this is that the PG quasars show no evidence for orientation-dependent effects and this is generally ascribed to the initial selection via ultra-violet excess. However, supporting evidence for PG 1407+263 being close to pole-on is the large velocity dispersion of its emission line gas  $\approx 10,000 \text{ km s}^{-1}$  (McDowell et al. 1995), indicating that we may be looking directly into the inner part of the broad-line region.

KMB thanks the Royal Society for a University Research Fellowship. AJB gratefully acknowledges support from NSF grant AST-0116558 (Combined Array for Research in Millimeter-wave Astronomy). The VLBA and VLA are facilities of the NRAO operated by AUI, under co-operative agreement with the NSF. We would like to thank the UKIRT service programme, and Dr Paul Hirst especially, for help in obtaining the UFTI data.

## REFERENCES

- Beasley A.J. and Conway J.E. 1995 in *Very Long Baseline Interferometry and the VLBA*, Astr. Soc. Pac. Conf. Ser. Vol. 82, Zensus, J.A., Diamond, P.J. and Napier, P.J. eds 328
- Bicknell G. V., Dopita M. A., Tsvetanov Z.I. & Sutherland R.S., 1998, ApJ, 495, 680
- Blundell K.M. & Beasley A.J., 1998a, MNRAS, 299, 165
- Blundell K.M. & Beasley A.J. 1998b, BAAS, 30, 1418
- Blundell K.M., Beasley A.J., Lacy M. & Garrington S.T., 1996, ApJ, 468, L91
- Blundell K.M. & Rawlings S. 2000, AJ, 119, 1111
- Blundell K.M. & Rawlings S. 2001, ApJ, 562, L5
- Brunthaler, A., et al, A&A, 2000, 357, L45
- Bridle A.H. & Perley R.A. 1984, ARA&A, 22, 319
- de Ruiter H., Parma P., Fanti C. & Fanti R., 1990, A&A, 227, 351
- Falcke H., Patnaik A.R. & Sherwood W., 1996, ApJ, 473, L13
- Fanaroff, B.L. & Riley, J.M. 1974, MNRAS, 167, 31P
- Gómez J. L., Marscher A. P., Alberdi A., Jorstad S. G. & Garcia-Miro C., Science, 289, 2317
- Hough D.H. et al., 1999, ApJ, 511, 84
- Kellermann, K.I., Sramek, R., Schmidt, M., Shaffer, D.B. and Green, R. 1989, AJ, 98, 1195
- McDowell J.C., et al, 1995, ApJ, 450, 585
- Miller L., Peacock, J.A. and Mead A.R.G. 1990, MNRAS, 244, 207
- Miller P., Rawlings S. and Saunders R. 1993, MNRAS, 263, 425
- Schmidt M. & Green R.F., 1983, ApJ, 269, 352
- Sopp H.M. and Alexander P. 1991a, MNRAS, 251, L14
- Sopp H.M. and Alexander P. 1991b, MNRAS, 251, 112
- Willott C.J., Rawlings S., Blundell K.M. & Lacy M., 1999, MNRAS, 309, 1017